Dust in Protoplanetary Disks: Properties and Evolution

Antonella Natta and Leonardo Testi
Osservatorio Astrofisico di Arcetri

Nuria Calvet
University of Michigan

Thomas Henning
Max Planck Institute for Astronomy, Heidelberg

Rens Waters
University of Amsterdam and Catholic University of Leuven

David Wilner
Harvard-Smithsonian Center for Astrophysics

We review the properties of dust in protoplanetary disks around optically visible pre-main-sequence stars obtained with a variety of observational techniques, from measurements of scattered light at visual and infrared wavelengths to mid-infrared spectroscopy and millimeter interferometry. A general result is that grains in disks are on average much larger than in the diffuse interstellar medium (ISM). In many disks, there is evidence that a large mass of dust is in grains with millimeter and centimeter sizes, more similar to "sand and pebbles" than to grains. Smaller grains (with micrometer sizes) exist closer to the disk surface, which also contains much smaller particles, e.g., polycyclic aromatic hydrocarbons. There is some evidence of a vertical stratification, with smaller grains closer to the surface. Another difference with ISM is the higher fraction of crystalline relative to amorphous silicates found in disk surfaces. There is a large scatter in dust properties among different sources, but no evidence of correlation with the stellar properties, for samples that include objects from intermediate to solar mass stars and brown dwarfs. There is also no apparent correlation with the age of the central object, over a range roughly between 1 and 10 m.y. This suggests a scenario in which significant grain processing may occur very early in the disk evolution, possibly when it is accreting matter from the parental molecular core. Further evolution may occur, but not necessarily rapidly, since we have evidence that large amounts of grains, from micrometer to centimeter size, can survive for periods as long as 10 m.y.

1. INTRODUCTION

Young stars are surrounded by circumstellar disks made of gas and dust. Some of these disks will form planets, and one of the current open questions is to understand which disks will do it, which will not, and why. In this chapter, we will refer to all circumstellar disks as *protoplanetary*, even if some (many) may only have the potential to evolve into a planetary system, and some (many) not even that.

The mass of protoplanetary disks is dominated by gas, but the solid component (dust grains) is of great importance. Observations of light scattered on dust grains and their thermal emission remain key diagnostic tools for detecting disks and characterizing their structure. Dust grains play an active role in determining the thermal and geometrical structure of disks because their opacity dominates over the gas opacity whenever they are present. Furthermore, grains shield the disk midplane from energetic radiation, thereby influencing the ionization structure, possibly leading to a "dead" zone where the magneto-rotational instability cannot operate. The formation of dust grains is a phase transition that provides solid surfaces important for chemical reactions and the freeze-out of molecular components such as CO and H_2O in the colder parts of disks. Finally, the solid mass of the disks is important because dust grains are the building blocks for the formation within the disk of planetesimals and eventually planets.

Grains in protoplanetary disks are very different from grains in the diffuse interstellar medium (ISM); their properties change from object to object and we believe that in each object they evolve with time. Without a comprehensive understanding of dust properties and evolution, many disk properties cannot be understood. An immediate example is the determination of disk solid masses from millimeter

continuum emission, which requires knowledge of the dust absorption coefficient for a specific grain composition and structure, and of the grain temperature.

Protoplanetary disks interest us also because they are the place where planets form. Grains are thought to be the primary building blocks on the road to planet formation, and the continuing and growing interest in this field is largely motivated by the need to understand the diversity of extrasolar planetary systems and reasons for this diversity. Earlier reviews by *Weidenschilling and Cuzzi* (1993) and *Beckwith et al.* (2000) in *Protostars and Planets III* and *IV* summarize what was known at the time. Since *Protostars and Planets IV* we have seen a lot of progress in our knowledge of grain properties in disks, thanks to high-resolution data provided by infrared (IR) long-baseline interferometry, the high sensitivity of Spitzer and groundbased 10 m-class telescopes, millimeter interferometers such as PdB and OVRO, and the VLA capabilities at millimeter wavelength. Data now exist for a large number of disks, around stars with very different mass and luminosity, from intermediate-mass objects (Herbig AeBe stars, hereafter referred to as HAeBe) to T Tauri stars (TTS) and brown dwarfs (BDs). On the theoretical side, there is a revived effort in modeling grain processing in disks (via coalescence, sedimentation, fragmentation, annealing, etc.) and its relation with the chemical and dynamical evolution of the gas. Although it is still very difficult to integrate observations and theory in a quantitative description of disk evolution, we can expect major advances in the near future.

In this review, we concentrate on observational evidence for grain evolution with a special emphasis on grain growth and mineralogy. As already mentioned, grain properties and their distribution within the disk affect many observable quantities. These aspects will be covered in other chapters of this book, and we will concentrate on observations that measure directly the grain physical and chemical structure. Prior to that, we will review very briefly the most important processes that control the grain properties (section 2). We will then outline the various observational techniques and their limitations (section 3), discuss evidence for grains of different size, from polycyclic aromatic hydrocarbons (PAHs; section 4) to micrometer size (section 5) and centimeter size (section 6). We will discuss grain mineralogy in section 7. Section 8 will summarize the main conclusions one can derive from the observations and outline some of the open questions we need to address in the future.

2. GRAIN GROWTH: WHY AND HOW

Grains in the ISM are very likely a mixture of silicates and carbons, with a size distribution from ~100 Å to maximum radii of ~0.2–0.3 μm. Smaller particles, most likely PAHs and very small carbonaceous grains, are also present (e.g., *Draine,* 2003). The composition of dust in molecular clouds is similar. Models of dust evolution in collapsing cores (*Krügel and Siebenmorgen,* 1994; *Ossenkopf and Henning,* 1994; *Miyake and Nakagawa,* 1995) predict only minor changes, as confirmed by the observations of Class 0 and Class I objects (e.g., *Beckwith and Sargent,* 1991; *Bianchi et al.,* 2003; *Kessler-Silacci et al.,* 2005).

Major changes occur once dust is collected in a circumstellar disk, where the pristine interstellar grains may grow from submicrometer-sized or even smaller particles, to kilometer-sized bodies (planetesimals), and eventually planets. This process is driven by coagulation of smaller particles into larger and larger ones, and has a long history of theoretical and laboratory studies, which it is not the scope of this paper to analyze. We refer for a critical discussion to the most recent reviews of *Henning et al.* (2006) and the chapter by Dominik et al. However, the relevance of the observations of grain properties we will discuss in the following is better understood in the context of grain growth and planetesimal formation models, which we will therefore briefly summarize here.

Grain growth to centimeter and even meter sizes is mainly driven by collisional aggregation, although gravitational instabilities may play a role in overdense dust regions. The relative velocities leading to such collisions are caused by the differential coupling to the gas motion (see, e.g., *Weidenschilling and Cuzzi,* 1993; *Beckwith et al.,* 2000). This immediately demonstrates that grain growth cannot be understood without a better characterization of the gas velocity field in disks, especially the degree of turbulence. For submicrometer-sized grains this is not a real issue and their growth by Brownian motion is reasonably well understood thanks to numerical simulations and extensive laboratory experiments (see, e.g., *Blum,* 2004, and the chapter by Dominik et al.). The relative velocities of grains in the 1–100-μm size range are on the order of 10^{-3} m/s to 10^{-4} m/s, low enough for sticking. The outcome of this early growth process is a relatively narrow mass distribution function with fractal aggregates having open and chain-like structures.

While growing in mass, particles also start to sediment [due to the vertical component of the stellar gravitational field (*Schräpler and Henning,* 2004; *Dullemond and Dominik,* 2005, and references therein)] and the relative velocities may eventually become higher, leading to the compaction of aggregates. Above the compaction limit, a runaway growth can be expected, where a few large aggregates grow by collisions with smaller particles. In this regime an exponential increase of mass with time can be expected. The coupling between sedimentation, grain growth, and structure of particles remains the next challenge for protoplanetary dust models, which have to deal with the transition from open to compact aggregates. For grains of boulder size (larger than 1 m), the relative velocities remain more or less constant at about 50 m/s, challenging growth models because this velocity is above the destruction threshold (but see *Wurm et al.,* 2005). Furthermore, such boulders are rapidly transported to the central star within a few hundred years. There are quite a number of proposals to solve the problem of the growth barrier, none with complete success yet.

In spite of the many uncertainties, the models converge on predicting that grains can grow to very large sizes and sediment under the effect of the stellar gravity, leaving a

population of smaller grains closer to the disk surface and of increasingly larger bodies toward the midplane. Grain growth should be much slower in regions further away from the star than in regions closer to it, which should be completely depleted of small grains. When only coagulation mechanisms are considered, small grains are removed very quickly, leading to the complete disappearance of the dusty disks on timescales much shorter than the age of observed disks. Mechanisms that replenish disks of small grains are clearly required, for example, aggregate fragmentation. Radial and meridian circulation can also play an important role in grain evolution.

The process of growth of grains from submicrometer to kilometer size we have described assumes that the original solid mass never returns to the gas phase. This may not be the case, as the temperatures in the inner disk are high enough to evaporate grains. If, over time, radial circulations carry close to the star most of the disk material, all the original solid mass is destroyed and condensed again in the disk. If so, the newly formed grains may be very different from those in the ISM, even if actual growth does not occur, or is important only above a certain (large) size. Gassification and recondensation of grains in the inner disk, coupled with strong radial drifts, has been suggested (*Gail,* 2004) as an explanation for the large fraction of crystalline grains seen in several disks (see section 7), and may also play an important role in determining the grain size distribution.

For a long time, the only test for planet formation theories was our own solar system. This has changed completely over the last decade, first with the discovery of the variety of planetary systems that can actually form, but also with a much better knowledge of the grain properties and distribution in disks that are the progenitors of planetary systems. Although our knowledge and understanding of this second aspect is still limited, and the answers to some key questions (e.g., which planetary systems will form and from which disks) elusive, we will show in the following that the observations may already provide important constraints to theory.

3. OBSERVATIONAL TECHNIQUES

Grain properties in disks can be explored with a variety of techniques and over a large range of wavelengths, from visual to centimeter. Before reviewing the results and their implication, it is useful to summarize briefly the capabilities and limitations of the different techniques.

The most severe limits to the characterization of grains in disks do not come from observational limits, such as spatial resolution or sensitivity (although these too can be a problem), but from the physical structure of disks. Their extremely high optical depth allows us to get information only on grains located in the $\tau = 1$ layer, which at optical and IR wavelengths contains a tiny fraction of the dust mass. Moreover, if one measures dust emission, the observed flux is strongly biased by the temperature dependence of the Planck function.

The only way to measure the properties of the bulk of the dust mass is to go to longer wavelengths, where an increasing fraction of the disk becomes optically thin. Interferometric observations at millimeter and centimeter wavelengths have provided the strongest evidence so far that most of the original solid mass in protoplanetary disks has grown to centimeter size by the time the central star becomes optically visible. However, one should remember that this technique is limited today by the sensitivity and resolution of existing millimeter interferometers. For example, studies of the radial dependence of the dust properties are still very difficult. Furthermore, even at these very long wavelengths, the regions of the disk closer to the star (typically up to a few AU) are optically thick, and thus this very interesting inner portion of the midplane remains inaccessible at all wavelengths.

The mid-IR spectral region, roughly between 3 and 100 μm, is rich in vibrational resonances of abundant dust species, silicates in particular. The spectral region between 3 and 20 μm also contains prominent PAH C-C and C-H resonances. The wavelength, spectral shape, and strength of the resonances are sensitive probes of the chemical composition, lattice structure, size, and shape of the particles. In disks around optically visible stars these dust features are generally seen in emission, having their origin in the optically thin surface layers, heated by the stellar radiation to temperatures higher than the disk midplane (e.g., *Calvet et al.,* 1991; *Chiang and Goldreich,* 1997; *Menshchikov and Henning,* 1997). Infrared spectroscopy roughly probes dust particles with sizes of up to a few micrometers (depending on material and wavelength) in the temperature range between 1500 and about 50 K. In protoplanetary disks, this implies that such spectra are sensitive to dust in the innermost regions, and in the surface layers of the disk only. No information is obtained about chemical and allotropic properties of large and/or cold dust grains.

The 10-μm spectral region deserves special attention because it is accessible from the ground, is available for high-spatial-resolution interferometric studies, and a fairly large body of data has been collected, covering a wide range of stellar mass and age. It contains the strongest resonances of both amorphous and crystalline silicates. The silicate emission bands have important but somewhat limited diagnostic value. First, the 10-μm spectral region probes grains of a certain temperature range, mostly between 200 and 600 K. Second, both the amorphous and crystalline silicate resonances near 10 μm only probe the presence of grains smaller than a few micrometers in size, the exact value depending on the dust species. This limits the diagnostic value of the 10-μm region to warm, small silicates mostly located on the disk surface in regions within ~10 AU for protoplanetary disks around HAe stars, ~0.5–1 AU for TTS, and ~0.1 AU for BDs.

At shorter wavelengths (visual and near-IR), scattering becomes important and one can observe scattered light extending to very large distances from the star (e.g., *McCaughrean et al.,* 2000). Multiwavelength images in scattered light can be used to derive grain properties over a large range of disk radii, but limited to a very narrow layer on the disk surface.

Interesting information on grain properties deeper in the disk can be obtained from edge-on disks (silhouette), seen as a dark lane against a luminous background. Information on dust properties can be obtained in favorable cases by studying the wavelength dependence of the dark lane absorption against the background of the scattered light at visual and near-IR wavelengths. Silhouette disks should have deep silicate features at 10 μm in absorption, which, contrary to the features in emission, sample the colder grains in the outer disk. Silicate absorption is observed in a few cases, but it is often difficult to exclude contamination from grains in the surrounding material.

Multiwavelength studies are obviously necessary to completely characterize the grain population in size, composition, and physical structure. So far, this cannot be done in disks, where observations at different wavelengths sample different regions of the disk. As we will describe in the following, there is clear evidence that grains of all sizes (from PAHs to centimeter-sized bodies at least) are present in disks. However, the information is always partial, and it is very difficult to get a global picture, for example, to measure the total mass fraction of grains of different size.

An additional caveat is that none of the techniques we have mentioned is sensitive to bodies larger than few centimeters. Kilometer-sized planetesimals can be detected through the dynamical perturbations they create, but the detection of meter-sized bodies is practically impossible.

4. THE SMALLEST PARTICLES: POLYCYCLIC AROMATIC HYDROCARBONS

Emission from transiently heated very small particles (at 3.3, 6.2, 7.7–7.9, 8.6, 11.3, and 12.7 μm, etc.) has been detected in many disk systems, mostly HAeBe stars (e.g., *Acke and van den Ancker,* 2004) and generally attributed to PAHs. For a long time, it has not been clear if the observed emission is from PAHs in the disks or from the reflection nebulosities associated with many HAeBe. There is now convincing evidence in favor of the disk origin.

Peeters et al. (2002), *van Diedenhoven et al.* (2004), and *Sloan et al.* (2005) have shown that in HAeBe stars the PAH features differ in shape and wavelength when compared to the ISM. *Meeus et al.* (2001) and *Acke and van den Ancker* (2004) found that the strength of the PAH bands correlates with the shape of the spectrum in the 10–60-μm region. Flared disks [i.e., with flux F_ν increasing with wavelength in the 10–60-μm range; group I in the *Meeus et al.* (2001) classification] have strong PAH features, while flat disks (i.e., with F_ν decreasing with wavelength in the 10–60-μm range; group II) have no or very weak emission. This trend has been analyzed by *Habart et al.* (2004a), who have computed disk models that include PAHs and have shown that the observed correlation between the strength of the PAH bands and the shape of the SED is well explained in terms of the solid angle the disk subtends as seen from the star. In a few stars, other features, at 3.43 and 3.53 μm, from transiently heated carbonaceous materials, possibly identified as nanodiamonds (*Guillois et al.,* 1999), have also been shown to have a disk origin (*Van Kerckhoven et al.,* 2002).

Recently, PAH and nanodiamond emission has been spatially resolved in several objects (*van Boekel et al.,* 2004b; *Ressler and Barsony,* 2003; *Habart et al.,* 2004b, 2006); the emitting region has a size consistent with disk model predictions (*Habart et al.,* 2004b, 2006; see Fig. 1). The emission of such transiently heated species (which are "hot" whenever excited) is much more extended than that of the adjacent continuum, emitted by larger grains in thermal equilibrium with the radiation field that rapidly become cool as the distance from the star increases. Using images in the features of PAHs and nanodiamonds it has been possible to measure disk inclination and position angle on the sky (*Habart et al.,* 2004b) at spatial scales of a few tens of AU.

The presence of very small particles on disk surfaces has a strong impact on the gas physical properties, since they contribute a large fraction of the gas heating via the photoelectric effect and may dominate the H_2 formation on grain surfaces. Polycyclic aromatic hydrocarbons are thus an essential ingredient of disk gas models (e.g., see the chapter

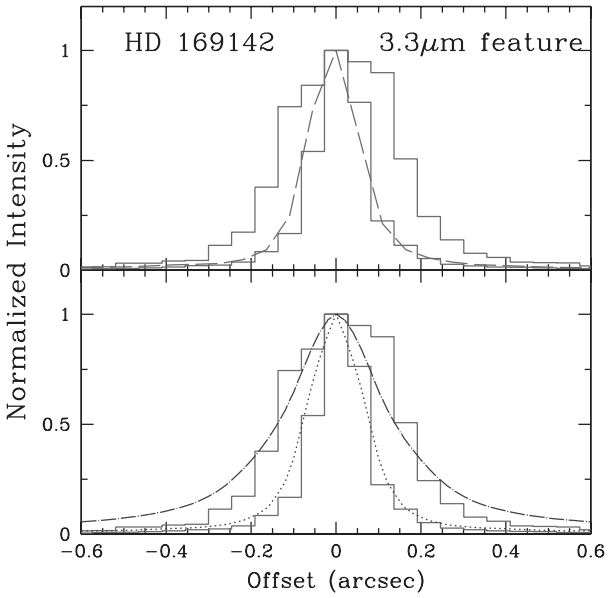

Fig. 1. Intensity profile of the 3.3-μm PAH feature in the HAe star HD 169142, observed with NAOS/CONICA on the VLT (*Habart et al.,* 2006). The top panel shows the intensity in the feature after continuum subtraction (thick solid line) and in the adjacent continuum (thin solid line); the dashed line plots the pointspread function as measured on a nearby unresolved star. The PAH feature is clearly spatially resolved, with FWHM size of 0.3 arcsec (roughly 40 AU at the distance of the star). The continuum is unresolved. The bottom panel compares the observations with disk model predictions for the feature (dot-dashed line) and the continuum (dotted line). Details of observations and calculations, including model parameters, are in *Habart et al.* (2004a, 2006).

by Dullemond et al.). However, the observations have severe limitations, as they can only probe matter at large altitudes above the disk midplane, so that we do not know if PAHs survive deeper into the disk; moreover, the intensity in the features decreases with radius, and is well below current observational capabilities for distances >40 AU (at least for the 3.3-μm feature).

There are also limitations in the current models, which need to explore a much wider range of parameters, both in disk and PAH properties.

5. FROM SUBMICROMETER- TO MICROMETER-SIZED GRAINS

5.1. Scattering and Polarization

Observations at visible and near-IR wavelengths of the dark disk silhouette seen against the background light scattered by the disk surface provide direct view of disks around young stars. The properties of the scattered radiation and the fraction of polarization can be used in principle to measure the size of the scattering grains. However, we know from laboratory work that particle sizing based on the angular distribution of scattered light or the measurement of polarization is not without problems and usually only works well for monodisperse distributions of spheres. In astronomical sources, the analysis of scattered radiation and polarization is even more complicated because it is not possible to obtain measurements for all scattering angles. In addition, polarization measurements are often technically challenging, which may explain why we only have limited data using this technique and grain size information from such observations is still scarce.

Scattering is well described by the 4×4 scattering matrix (Mueller matrix) transforming the original set of Stokes parameters into a new set after the scattering event. The matrix elements are angular-dependent functions of wavelength, particle size, shape, and material. For particles that are small compared with the wavelengths, the scattered light is partially polarized with a typical bell-shaped angular dependence with 100% polarization at a scattering angle of 90°. The polarization degree depends only on the scattering angle and not on particle size. This practically means that the radius of small spherical particles cannot be determined from scattering measurements.

For very small particles scattering does not vary a lot with direction. This changes drastically for larger spheres with more ripples and peaks in the scattering pattern, for which forward scattering becomes very important. In addition, the peak polarization decreases and moves to larger scattering angles. The very structured scattering pattern for large spheres is used for experimental particle sizing, but the characteristic ripples disappear if a grain size distribution is considered instead of a single size population. For very large spheres we again find smooth curves. Furthermore, nonspherical particles may behave very differently. We should also note that an ensemble of nonidentical scattering particles leads to depolarization of scattered light, adding to the complexity of our understanding of the polarization degree (in terms of grains sizes) of radiation coming from a disk. We refer to *Voshchinnikov and Krügel* (1999) for Mie calculations, demonstrating the effect of different grain sizes.

One may conclude that solving the inverse problem of determining grain sizes from scattering and polarization observations is hopeless. This is certainly not true. A growing number of objects are studied using multiwavelength imaging and polarization techniques. For our purposes, it is sufficient to note that, in all cases, the evidence points toward grain growth on the disk surface to sizes of up to a few micrometers; often, there is also evidence of sedimentation, i.e., that larger grains are closer to the disk midplane. Among the more recent studies, we note the work of *Lucas et al.* (2004), who nicely demonstrated the power of a detailed analysis of high-resolution imaging polarization data for the case of HL Tau. They found that silicate core-ice mantle grains with the largest particles having radii slightly in excess of 1 μm best fit the data. A similar study has been performed for the ring around GG Tau by *Duchêne et al.* (2004). They found again a slight increase in the grain size toward micrometer-sized grains, and evidence for a vertical stratification of dust. The surface layers, located ~50 AU above the ring midplane, contain dust grains that are consistent with being as small as in the ISM, while the region of the ring located ~25 AU from the midplane contains significantly larger grains (>1 μm). This stratified structure is likely the result of vertical dust settling and/or preferential grain growth in the densest parts of the ring. The first scattering measurements at mid-IR wavelengths obtained for the T Tauri star HK Tau B (*McCabe et al.,* 2003) showed similar results.

Evidence of growth of grains to sizes of up to a few micrometers and of a vertical stratification of grain sizes within the disk surface has also been inferred in silhouette disks in Taurus (*D'Alessio et al.,* 2001) and Orion (*Throop et al.,* 2001; *Shuping et al.,* 2003; see also *McCaughrean et al.,* 2000, and references therein) by studying the behavior with wavelength of the translucent edges of the dark lane.

5.2. Mid-Infrared Spectroscopy

High-quality mid-IR spectra are available for an increasing number of objects. First the Infrared Space Observatory (ISO) and now the Spitzer Space Telescope are providing us with data of a quality that could not be achieved from the ground, even if the spatial resolution is in both cases too low to resolve the emission. Spitzer spectra are becoming available in increasing number at the time we write, and we expect further improvement in the statistics and quality of the data, for low mass objects in particular. In the following, we provide a summary of the silicate properties, as derived from the available observations.

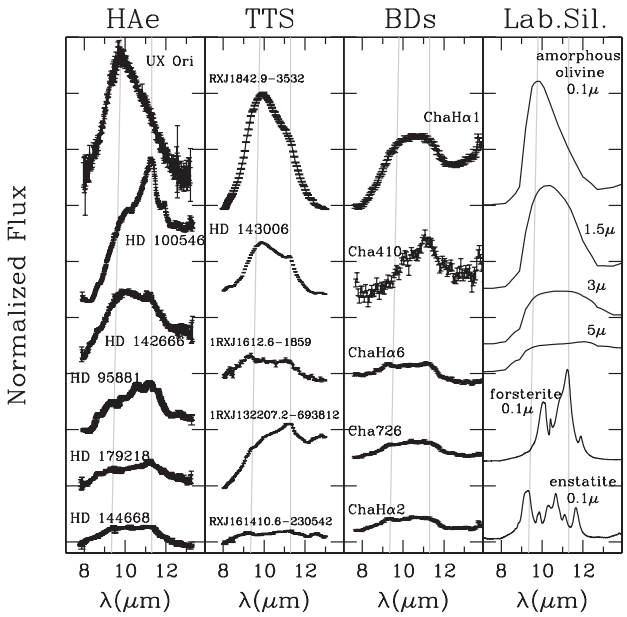

Fig. 2. Observed profiles of the 10-μm silicate feature. The first three panels (from left to right) show a selection of profiles for HAe stars (*van Boekel et al.,* 2005), TTS (Bouwman et al., in preparation), and BDs in Chamaeleon (*Apai et al.,* 2005). All the profiles have been normalized to the 8-μm flux and shifted for an easier display. In each panel, they have been ordered according to the F_{peak}/F_{cont} value. The dashed vertical lines show the location (at 9.8 μm) of the peak of small amorphous olivine (Mg_2SiO_4) and of the strongest crystalline feature of forsterite at 11.3 μm. Amorphous silicate grains of composition $Mg_{2x}Fe_{2-2x}SiO_4$, generally with $x \ll 1$ have the same composition of olivines, and are often referred to as "amorphous olivines." Although this is not correct (olivine is crystalline), we will sometime use this definition. The panel to the far right shows for comparison a selection of profiles of laboratory silicates: starting at the top, amorphous olivine with radius 0.1, 1.5, 3, and 5 μm, as labeled. In all cases, we have added the same continuum (30% of the peak of the 0.1-μm amorphous olivine), and normalized as the observed profiles. The two bottom curves show the profile of small crystalline grains, forsterite (Mg_2SiO_4) and enstatite ($MgSiO_3$), respectively; larger crystalline grains have broader and weaker features (e.g., *van Boekel et al.,* 2005). Several of the features displayed by crystalline silicates can be identified in some of the observed spectra.

Most of the information is obtained from observations of the 10-μm emission feature. The spectra show a large variation in the strength and shape of this feature, for objects of all mass, from HAe stars to TTS and BDs. Figure 2 plots a representative selection of HAe stars, TTS, and BDs, which shows the variety of observed profiles. In some cases, the shape of the feature is strongly peaked at about 9.8 μm, as for small (≪1 μm) amorphous grains in the ISM. In other objects, the feature is very weak with respect to the continuum, and much less peaked. In other cases, many narrow features, typical of crystalline silicates, are clearly visible, superimposed on the smoother and broader amorphous silicate emission. These features will be discussed in detail in section 7. In spite of these large variations, there is a general trend, valid for objects of all mass, first identified by *van Boekel et al.* (2005), who noted that the shape and strength of the silicate band are correlated, so that weaker features are also flatter. This is consistent with the growth of silicate grains from submicrometer to micrometer sizes. If grains grow further, the silicate emission disappears; there are in fact a few objects that show no silicate emission, most likely because *all* small silicates have been removed (e.g., *Meeus et al.,* 2003).

A useful way to summarize the properties of the 10-μm feature of a sample of objects is shown in Fig. 3. For each object, the shape of the 10-μm silicate emission feature is characterized by two parameters, the ratio of the flux at the peak of the feature over the continuum (F_{peak}/F_{cont}) and the ratio of the continuum subtracted 11.3 μm over the 9.8-μm flux. Amorphous silicates of increasing size have weaker and flatter features (cf. Fig. 2), with values of F_{peak}/F_{cont} decreasing from 3–4 (for sizes ≪1 μm) to ~1, for grains

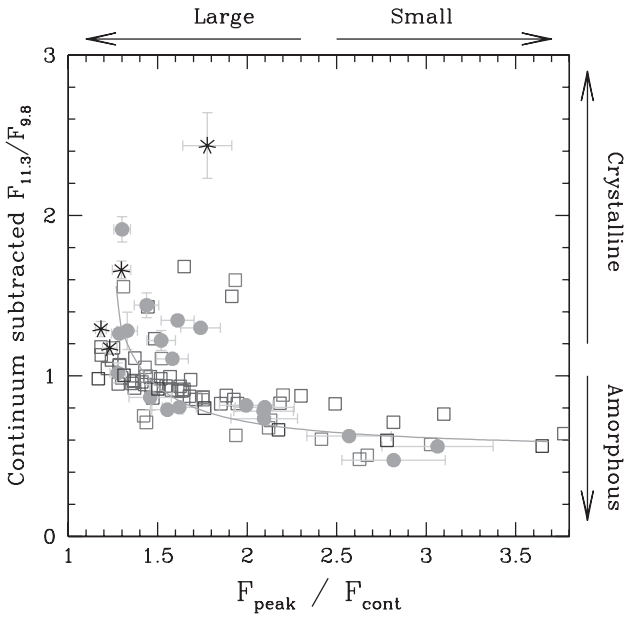

Fig. 3. The ratio of the continuum-subtracted flux at 11.3 μm over that at 9.8 μm ($F_{11.3}/F_{9.8}$) is plotted as function of flux at the peak of the 10-μm feature over the continuum, F_{peak}/F_{cont}. Open and filled symbols show the observations for HAe stars [filled dots, *van Boekel et al.* (2005)], TTS [squares, *Kessler-Silacci et al.* (2006); Bouwman et al. (in preparation); *Przygodda et al.* (2003)], BDs [stars, *Apai et al.* (2005)]. All the data but those of *Kessler-Silacci et al.* (2006) and Bouwman et al. (in preparation) have been reanalyzed by *Apai et al.* (2005) in a homogeneous way. Error bars are shown when available in the literature. The solid curve shows the result for a dust model that includes amorphous olivine of two sizes (1 and 10 μm) in proportion varying from all 1 μm (extreme right) to all 10 μm (extreme left), and an additional contribution of a 2% mass fraction of 0.1-μm forsterite grains (from J. Bouwman, personal communication, 2005); the same continuum (25% of the peak flux of the smallest grains) is added to all model spectra.

larger than few micrometers. At the same time, the ratio $F_{11.3}/F_{9.8}$ increases from ~0.5–0.6 to ~1. Larger values of the ratio $F_{11.3}/F_{9.8}$ are due to a significant contribution from forsterite (i.e., crystalline Mg_2SiO_4).

Note that the ratio F_{peak}/F_{cont} depends not only on grain cross section but also on other quantities (e.g., the disk inclination and geometry) that affect feature and continuum emission differently (e.g., *Chiang and Goldreich,* 1999). Also, changes in grain properties other than size [e.g., porosity (see *Voshchinnikov et al.,* 2006; *Min et al.,* 2006)] can reproduce part of the observed trend, and make the simple analysis in terms of grain size more uncertain. However, the interpretation of the 10-μm feature profiles in terms of growth of the grains in the disk surface is convincing, and in agreement with the results from other kinds of observations discussed in section 5.1.

Additional information will be derived in the future from the properties of the weaker 20-μm silicate band, which samples slightly larger grains, and regions on the disk surface further away from the star. Spitzer spectra are becoming available for a rapidly growing number of objects, and the first results seem to confirm the results obtained from the 10-μm feature analysis (*Kessler-Silacci et al.,* 2006; Bouwman et al., in preparation).

6. GROWTH TO CENTIMETER-SIZED GRAINS

As discussed in section 3, at (sub-)millimeter wavelengths and beyond the dust emission in disks begins to be moderately optically thin. At these wavelengths it is thus possible to probe the bulk of the dust particles, which are concentrated in the disk midplane. The spectral energy distribution of the continuum emission can be directly related to the dust emissivity, which in turn is related to the grain properties. The variation of the dust opacity coefficient per unit mass with frequency, in the millimeter wave range, can be approximated to relatively good accuracy by a power law $k \sim \lambda^{-\beta}$. The value of the β exponent is directly related to the dust properties, in particular the grain size distribution and upper size cutoff; in the limit of dust composed only of grains much larger than the observing wavelength, the opacity becomes gray and $\beta = 0$.

It has been known for many years that pre-main-sequence disks have (sub-)millimeter spectral indices α ($F_\nu \propto \lambda^{-\alpha}$) shallower than prestellar cores and young protostars (*Beckwith and Sargent,* 1991). If the disk emission is optically thin and $h\nu/kT_d \ll 1$, the observed values of α would translate very simply in opacity power law indices $\beta = \alpha - 2$; with observed typical values of $\alpha \leq 3$, this would imply $\beta \sim 1$ or lower. This immediately suggests that disk grains are very different from ISM grains, which have $\beta \sim 1.7$ (*Weingartner and Draine,* 2001).

This result, however, has been viewed with great caution, since the effect of large optical depth at the frequency of the observations cannot be ruled out for spatially unresolved observations. The extreme case of an optically thick disk made of ISM grains has $\alpha = 2$, the same value as an optically thin disk with very large grains, for which $\beta = 0$ (see, e.g., *Beckwith and Sargent,* 1991; *Beckwith et al.,* 2000). The combination of optical depth and grain properties can be disentangled if the emission is resolved spatially and the disk size at the observed wavelength is measured (see, e.g., *Testi et al.,* 2001, 2003).

There are now several disks whose millimeter emission has been imaged with interferometers. A major step forward has come from the use of 7-mm VLA data, which, in combination with results at shorter wavelengths (1.3 and 2.6 mm) with PdB and OVRO, provides not only high spatial resolution and larger wavelength range (minimizing the uncertainties on α), but also the possibility of probing population of grains as large as a few centimeters. Additionally, the VLA at centimeter wavelengths has been useful to check whether the dust emission at shorter wavelength is contaminated by free-free emission (e.g., *Testi et al.,* 2001; *Wilner et al.,* 2000; *Rodmann et al.,* 2006). We summarize in Fig. 4 the results for the objects with 7-mm measurements from

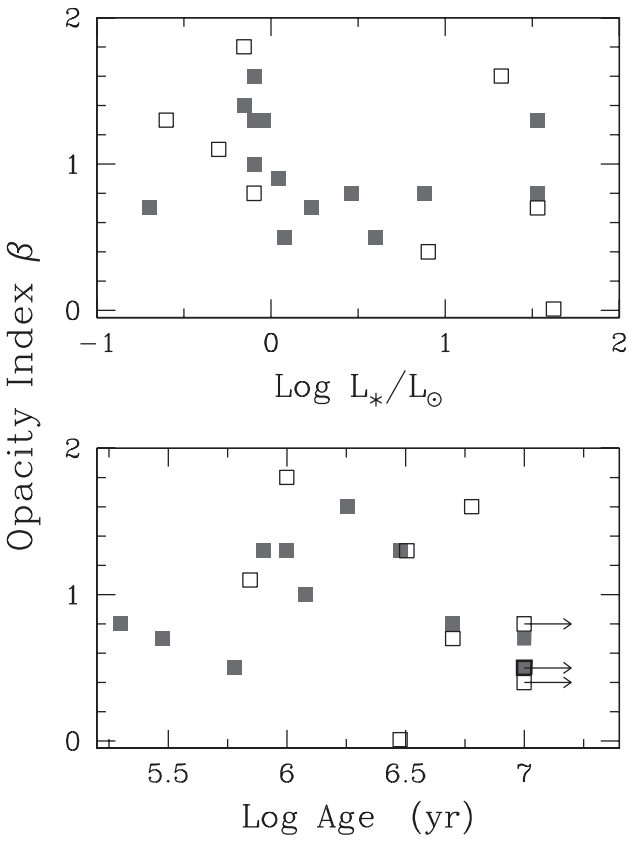

Fig. 4. The values of the millimeter opacity index β ($\kappa \propto \lambda^{-\beta}$) plotted as a function of the stellar luminosity (top panel) and of the stellar age (bottom panel); data from *Natta et al.* (2004a) and *Rodmann et al.* (2006). Filled squares are objects where the disk millimeter emission has been spatially resolved, open squares are objects that have not been observed with high spatial resolution, or that were found to be not resolved with the VLA (resolution ~0.5 arcsec).

Natta et al. (2004a) and references therein and *Rodmann et al.* (2006). For these objects, the contribution from gas emission has been subtracted from the millimeter emission, and the spectral index α has been computed over the wavelength interval 1.3–7 mm; in three cases the 7-mm flux is an upper limit, once the gas emission has been subtracted from the total. The values of β have been derived fitting disk models to the data. Note that these model-fitted β values are slightly larger than the optically thin determination $\beta = \alpha - 2$, typically by about 0.2. This difference is due to the fact that the emission of the inner optically thick disk, albeit small, is not entirely negligible. The uncertainty on the model-derived β is of about ±0.2 (*Natta et al.,* 2004a; *Rodmann et al.,* 2006. The figure shows also the results for those objects for which no resolved maps exist, but have measurements of the integrated flux at 7 mm. For these, β has been derived from the measured α assuming that the disk is larger than ~100 AU, sufficient to make the optically thick contribution small.

If we consider only the 14 resolved disks, which have all radii larger than 100 AU, β ranges from 1.6 (i.e., very similar to the ISM value), to 0.5. Ten objects have $\beta \leq 1$, i.e., much flatter than ISM grains. The unresolved disks behave in a similar way; the extreme case is UX Ori, with $\beta \sim 0$. Unfortunately, the UX Ori disk has not been resolved so far; at the distance of ~450 pc, and, with an integrated flux at 7 mm of only 0.8 mJy (*Testi et al.,* 2001), it remains a tantalizing object. High and low values of β are found both for HAe stars and for TTS, and there is no apparent correlation of β with the stellar luminosity or mass. Similarly, we do not observe any correlation of β with the age of the star. This last quantity, however, is often very uncertain, and the observed sample limited.

Once we have established that the grains originally in the collapsing cores, for which $\beta \sim 1.7$–2, have gone through a large degree of processing, one wants to derive from β the properties of the actual grain population, and in particular its size. The properties of the millimeter opacity of grains of increasing size have been discussed by, e.g., *Beckwith et al.* (2000) and references therein. Figure 5 illustrates the behavior of β computed between 1 and 7 mm for a population of grains with size distribution $n(a) \propto a^{-q}$ between a_{min} and a_{max}. The index β is plotted as function of a_{max} for different values of q; in all cases, $a_{min} \ll 1$ mm. One can see that, for all values of q, as a_{max} increases β is first constant at the value typical of grains of size ≪1 mm, it has a strong and rather broad peak at $a_{max} \sim 1$ mm and decreases below the initial value for $a_{max} \gtrsim$ few mm. However, only for $q < 3$ does β go to zero for large a_{max}; for $q > 3$, the small grains always contribute to the opacity, so that β reaches an asymptotic value that depends on q and on the β of the small grains. For $q = 4$, the asymptotic value is practically that of the small grains.

The results shown in Fig. 5 have been computed for compact segregated spheres of olivine, organic materials, and water ice (*Pollack et al.,* 1994). The exact values of β depend on grain properties, such as their chemical composition, geometrical structure, and temperature (e.g., *Henning et al.,* 1995); examples for different grain models can be found, e.g., in *Miyake and Nakagawa* (1993), *Krügel and Siebenmorgen* (1994), *Calvet et al.* (2002), and *Natta et al.* (2004a). However, these differences do not undermine the general conclusion that the observed spectral indices require that grains have grown to sizes much larger than the observing wavelengths (e.g., *Beckwith et al.,* 2000, and references therein; *Draine,* 2006). To account for the observations that extend to 7 mm, objects with $\beta \sim 0.5$–0.6 need a distribution of grain sizes with maximum radii of a few centimeters, at least. The minimum grain radii are not constrained, and could be as small as in the ISM; however, the largest particles need to contribute significantly to the average opacity, which implies that the grain size distribution cannot be steeper than $n(a) \propto a^{-(3-3.5)}$; in any case, the large grains contain most of the solid mass. A detailed analysis can be found in, e.g., *Natta and Testi* (2004).

Of the objects observed so far, TW Hya is a particularly interesting case. Millimeter observations can be fitted well

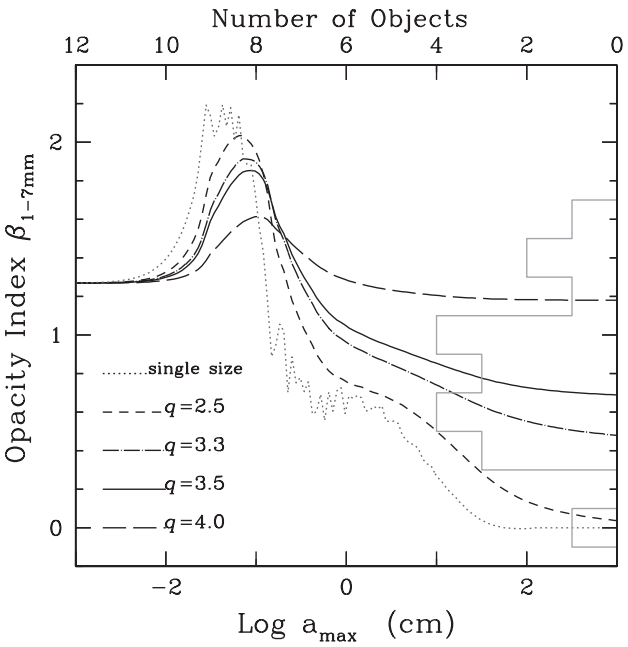

Fig. 5. Opacity index β for grains with a size distribution $n(a) \propto a^{-q}$ between a_{min} and a_{max}. The index β is computed between 1 and 7 mm for compact segregated spheres of olivine, organic materials, and water ice (*Pollack et al.,* 1994), and plotted as function of a_{max}. Different curves correspond to different values of q, as labeled. In all cases, $a_{min} \ll 1$ mm. The dotted curve shows β for grains with single size a_{max}. The histogram on the right shows the distribution of the values of β derived from millimeter observations (see Fig. 4). About 60% of the objects have $\beta \leq 1$, and $a_{max} \geq 1$ cm. Different dust models give results that are not very different (e.g., *Natta and Testi,* 2004).

with models that include grain growth up to 1 cm (*Calvet et al.,* 2002; *Natta and Testi,* 2004; *Qi et al.,* 2004). However, this is probably an underestimation of the maximum grain sizes in this disk. *Wilner et al.* (2005) have demonstrated that the 3.5-cm emission of this object, contrary to expectations, is not dominated by gas emission, but rather by thermal emission from dust grains in the disk, and that a population of particles as large as several centimeters residing in the disk is needed to explain both the long-wavelength SED and the spatial distribution of the 3.5-cm emission.

The result that dust particles have grown to considerable sizes, in fact to "pebbles," is thus a solid one and verified in many systems. So far, it has been derived as a "global" property of the dust grain population of the disk. In order to constrain dust growth models, the next logical step is to check for variation of dust properties as a function of radius. A first attempt at this type of study is shown in Fig. 6. High angular resolution and high signal-to-noise 7-mm (VLA) and 1.3-mm (PdBI) maps of the HD 163296 system have been combined to reconstruct the millimeter spectral index profile as a function of radius. The result suggests that the spectral index varies as a function of radius from $\alpha \sim 2.5$ in the inner ~60 AU to $\alpha \sim 3.0$ in the far outer disk. If interpreted as differential grain growth, this result implies that the outer disk contains less-evolved particles than the inner disk.

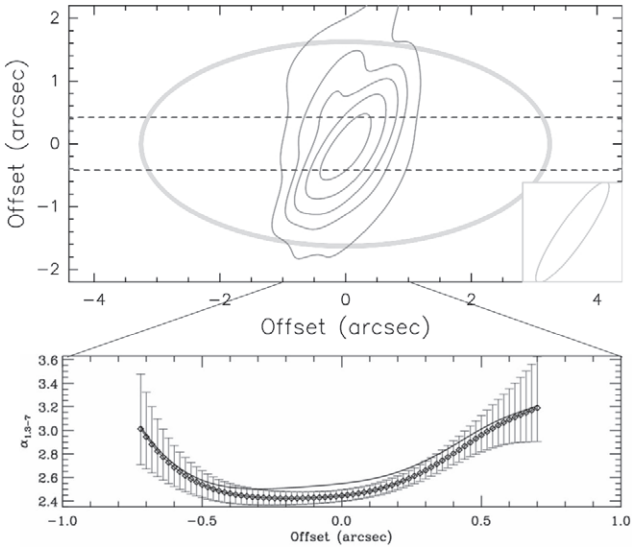

Fig. 6. The top panel shows the IRAM-PdBI contour map of the 1.3-mm emission from the disk, and the approximate shape and size of the scattered light disk as detected with HST/STIS. The images have been rotated so that the major axis of the disk is aligned with the abscissa of the plot. The spatial resolution of the millimeter observations is shown by the ellipse in the lower right box of the upper panel. In the bottom panel the diamonds with error bars show the variation along the disk major axis of the continuum spectral index measured between 1.3 and 7 mm. In the same panel, the solid line shows the values of the spectral index when a correction for the maximum possible gas contribution is applied to the 7-mm observations. The data suggest a variation of the spectral index as a function of disk radius. If interpreted as a variation of the grain properties, they indicate that larger grains are found in the inner ($r \leq 60$ AU) regions of the disk, while the grains in the outer disk may still be in a less-evolved stage.

7. MINERALOGY

The ISO and the latest generation of mid-IR spectrographs on large groundbased telescopes have revealed the presence of many new dust species, in addition to amorphous silicates, in the protoplanetary disks surrounding pre-main-sequence stars. The position and strength of the observed emission bands match well those of Mg-rich and Fe-poor crystalline silicates of the olivine ($Mg_{2x}Fe_{2-2x}SiO_4$ and pyroxene $Mg_xFe_{1-x}SiO_3$ families, in particular their Mg-rich end members forsterite and enstatite respectively (x = 1). Apart from these components, evidence for FeS and SiO_2 was also found (*Keller et al.,* 2002). Spitzer is now providing similar results for stars of lower mass, TTS and BDs.

The presence of these dust species in protoplanetary disks implies substantial processing (chemical and physical) of the dust because their abundance, relative to that of amorphous silicates, is far above limits set for these species in the interstellar medium (e.g., *Kemper et al.,* 2004). Therefore, these dust species must be formed sometime during the collapse of the molecular cloud core or in the accretion disk surrounding the young star. There are several possible mechanisms that may be responsible for grain processing, and it is quite likely that several contribute. In the innermost disk regions, where the dust temperature is above 1000 K, heat will induce a change of the grain lattice ordering (long-range ordering) from chaotic to regular (thermal annealing), leading to the transformation of amorphous silicates into crystalline ones (olivines and pyroxenes). Above about 1200–1300 K, chemical equilibrium processes will lead to vaporization and gas-phase condensation of silicates, mostly in the form of crystalline forsterite. Local high-energy processes (shocks, lightning) as well as radial mixing may increase substantially the amount of crystalline silicates in the cool outer regions of the disk. Note that thermal annealing of amorphous, presumably Fe-rich silicates would lead to Fe-rich crystalline silicates. Therefore the Fe content of crystalline silicates may be used as an indication of the chemical processing that has occurred (gas-phase condensation, annealing, local processes). In this context, we stress the importance of improving the still poorly constrained stochiometry of interstellar amorphous silicates, in particular the Fe/Mg and Mg/Si ratio.

The mineral composition of dust in protoplanetary disks can be compared directly to that of solar system comets, asteroids, and interplanetary dust particles (IDPs). Only one high-quality 2–200-μm spectrum of a solar system comet, Hale-Bopp, is available from ISO. The crystalline silicates

in Hale-Bopp are very Mg-rich and Fe-poor, similar to those in protoplanetary disks. Laboratory studies of IDPs of cometary origin also reveal the presence of Mg-rich crystalline silicates. The situation for asteroids is much more diverse. Apart from Mg-rich crystalline silicates, many asteroids show Fe-containing silicates, probably related to parent body processing or to nebular processing in the inner solar nebula.

7.1. Spatially Unresolved 10-Micrometer Spectra

Information on the abundance of crystalline silicates in a large sample of objects of different mass are derived from the shape of the 10-μm feature (mostly through the 11.3-μm forsterite peak) in spatially unresolved observations. Figure 2 shows how this feature can be prominent in stars of all mass, from HAeBe to brown dwarfs. Figure 3 shows how in many objects the flux at 11.3 μm is stronger than at 9.8 μm, where the emission of small amorphous silicates roughly peaks. A strong 11.3-μm peak is typical of profiles with a large component of crystalline silicates, in addition to the amorphous ones. This interpretation has been confirmed by the presence of crystalline features at longer wavelengths, when the data are available. Contamination from the 11.3-μm PAH feature has been ruled out in many cases, from the absence of the other PAH features at shorter wavelengths (see, e.g., *Acke and van der Ancker,* 2004).

A determination of the fractional mass abundance of the crystalline silicates has been derived by various authors fitting the observed profiles with mixtures of grains of different composition (typically, olivines and pyroxenes), size (from submicrometer to few micrometers) and allotropic state (amorphous and crystalline). In general, the models assume a single temperature for all grains and that the emission is optically thin. These assumptions, and the limited number of dust components that are included in models, make the estimates very uncertain. However, the results are interesting. For HAeBe stars, *van Boekel et al.* (2005) find that crystalline silicates are abundant only when the amorphous silicate grain population is dominated by large (≥1.5 μm) grains. In Fig. 3, there are no points with 11.3/9.8 ratio ≥ 1 and large values of F_{peak}/F_{cont}. The fraction of grains that is crystalline ranges from 5% (detection limit) to ~30%. Note that grains larger than few micrometers are not accounted for; if crystalline silicates are mostly submicrometer in size, while the amorphous species have a much broader distribution, the degree of crystallinity can be much lower than current estimates. This seems to be the case in Hale-Bopp (*Min et al.,* 2005), and may occur in protostellar disks as well. In addition, the derived crystalline/amorphous abundances are spatially averaged values; there are likely strong radial gradients in crystallinity (see below). As more data for lower-mass objects become available, we see that they show a similar trend, although relatively high crystallinity and relatively few large amorphous grains have been seen in one very low mass TTS (e.g., *Sargent et al.,* 2005). Recent Spitzer data for brown dwarfs in ChaI show that objects of very low mass also have a large fraction of crystalline silicates, from 9% to about 50% (*Apai et al.,* 2005).

As far as the chemical composition of the silicates is concerned, there are some general trends, showing that crystalline pyroxene grains can be found in disks with relatively large fractions of forsterite and silica, but they are typically not found in disks with small fractions of forsterite and silica (*van Boekel et al.,* 2005; *Sargent et al.,* 2006).

7.2. Spatially Resolved Spectroscopy

The advent of spectrally resolved mid-IR interferometry using large baselines at the Very Large Telescope Interferometer (VLTI) has made it possible for the first time to study the nature of the dust grains on AU spatial scales. The MIDI instrument at the VLTI has been used to study the innermost regions of HAeBe star disks. *van Boekel et al.* (2004a) (see Fig 7) show that the inner 1–2 AU of the disk surface surrounding three HAe stars is highly crystalline, with between 50% and 100% of the small silicates being crystalline. However, crystalline silicates are also present at larger distance, with a wide range of abundances. A similar behavior is found in other objects observed with MIDI

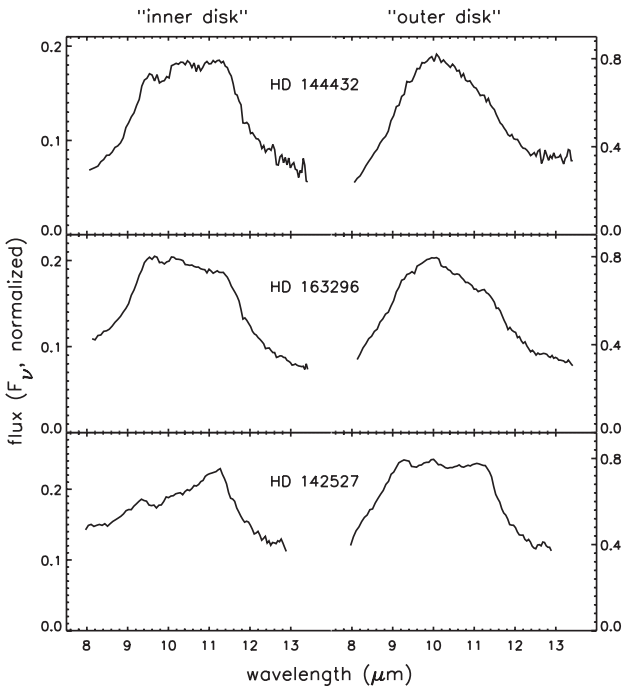

Fig. 7. Comparison of the silicate profiles from the inner (1–2 AU) and outer (2–20 AU) disk in three HAe stars (*van Boekel et al.,* 2004a). The data have been obtained with the mid-IR interferometric instrument MIDI on the VLTI. The comparison shows that, for all three stars, the crystalline features are much stronger in the inner than in the outer disk.

(Leinert et al., in preparation). Clearly, large star-to-star variations in the amount and distribution of the crystalline silicates exist, but it seems that crystalline grains are relatively more prominent in the inner than in the outer disk. Note that, because silicate emission from cold grains become very weak, in this case "outer" refers to warm regions of the disk between 2 and 20 AU at most (*van Boekel et al.,* 2004a).

In the star with the highest crystallinity, HD 142527, the observations suggest a decrease in the ratio between forsterite and enstatite with increasing distance from the star. Such a trend in the nature of the crystals with distance is predicted by chemical equilibrium and radial mixing models (*Gail,* 2004). The innermost disk is expected to contain mostly forsterite, while at larger distance from the star a conversion from forsterite to enstatite takes place. Thermal annealing produces both olivines and pyroxenes, with a ratio depending on the stochiometry of the amorphous material accreted from the parent molecular cloud. *van Boekel et al.* (2004a) also find evidence for a decrease of the average grain size with distance from the star, suggesting that grain aggregation has proceeded further in the innermost, densest disk regions.

7.3. TW Hya Systems

A number of objects with distinct signs of evolution of their inner disk has been identified in the last decade. These objects with "transitional" disks are characterized by spectral energy distributions (SEDs) with a flux deficit in the near-IR relative to the median SED of classical T Tauri stars in Taurus [a proxy for the expected emission from optically thick disks (see *D'Alessio et al.,* 1999)], while at longer wavelengths fluxes are comparable or sometimes higher than the median SED of Taurus. Groundbased near- and mid-IR photometry combined with IRAS fluxes allowed the identification of objects with these properties in Taurus (*Marsh and Mahoney,* 1992; *Jensen and Mathieu,* 1997; *Bergin et al.,* 2004) and in the TW Hya association (*Jayawardhana et al.,* 1999; *Calvet et al.,* 2002). However, instruments onboard Spitzer are providing a much better view of the characteristics and frequencies of these objects (*Uchida et al.,* 2004; *Forrest et al.,* 2004; *Muzerolle et al.,* 2004; *Calvet et al.,* 2005; *Sicilia-Aguilar et al.,* 2006). The inner disk clearing may be related to photoevaporation of the outer disk by UV radiation (*Clarke et al.,* 2001). However, transitional disks have now been found in brown dwarfs (*Muzerolle et al.,* 2006), for which the UV supply of energy is negligible. An alternative explanation is that a planet has formed and carved out a gap in the disk; hydrodynamical simulations seem to support this view (*Rice et al.,* 2003; *Quillen et al.,* 2004).

The 10-m.y.-old TW Hya was the first of these objects analyzed in detail. The peculiar SED of this object (*Calvet et al.,* 2002; *Uchida et al.,* 2004) can be understood by an optically thick disk truncated at ~4 AU; the wall at the edge of this disk is illuminated directly by stellar radiation, producing the fast rise of emission at wavelengths >10 μm. The region encircled by this wall is not empty. For one thing, it has gas, because the disk is still accreting mass onto the star (*Muzerolle et al.,* 2000). In addition, this inner region contains ~0.5 $M_{\leftmoon}$ of micrometer-sized particles, responsible for the small near-IR flux excess over photospheric emission. This dust is also responsible for the strong silicate feature at 10 μm, which allows us to examine the conditions of the dust in the inner disk (*Calvet et al.,* 2002). The profile of the 10-μm feature, integrated over the disk, is typical of amorphous silicates with sizes of ~2 μm (*Uchida et al.,* 2004), with a very low content of crystalline silicates, <2% fraction by mass (*Sargent et al.,* 2005). However, interferometric observations with MIDI resolve the feature from the inner disk [within ~1 AU (Leinert et al., in preparation; see chapter by Millan-Gabet et al.)], showing clearly the 11.3-μm peak typical of forsterite, while the uncorrelated profile is very similar to that measured with single-dish instruments.

Sargent et al. (2006) have analyzed the dust content of a number of transitional disks, in addition to TW Hya. They find, averaged over the whole disk, a very low content of crystalline silicates. In contrast, there is a large spread of the crystalline silicate fraction (from 0.3% to 20% in mass) in their sample of objects with optically thick inner disks.

These results support the idea that disks accumulate crystalline silicate grains in their innermost regions and that radial mixing transports outward some fraction of this material, with an efficiency that decreases with radius. In transitional disks, a large fraction of the region within approximately a few AU is cleared out, leaving only material with low crystalline content. Spatially resolved observations of the innermost regions are needed to detect the small amount of remaining grains, with their higher crystallinity.

8. SUMMARY AND OPEN PROBLEMS

8.1. Evidence of Grain Growth

The results we have discussed come from a variety of techniques, including optical, near- and mid-IR imaging, mid-IR spectrometry, and millimeter interferometry. All the data show clear evidence that grains in protoplanetary disks differ significantly from grains in the diffuse ISM and in molecular clouds. They are much larger on average, and there is increasing support for a scenario in which grains grow and sediment toward the disk midplane. On the surface of the disk, within a few tens of AU from the star, we know that in most cases silicates have grown to sizes of few micrometers, although much smaller particles (PAHs) may be present as well, and there are hints of vertical stratification (at several scale heigths from the midplane) of these micrometer-sized grains from studies of scattered light and silhouette disks. We have evidence from millimeter interferometry that, if we consider not only grains on the disk

surface but the bulk of the dust mass, in many disks grain growth has not stopped at micrometer sizes, but there is a dominant population of "sand and pebbles," millimeter and centimeter grains. In addition to vertical gradients of grain sizes, there is also evidence that radial gradients of grain properties exist, as shown by mid-IR interferometry, absorption mid-IR spectra of silhouette disks, and millimeter images at different wavelengths, as discussed before. Grains in the very outer disk seem to be less processed than grains closer to the star.

One important aspect to keep in mind is that not all the objects show evidence of processed grains: In some stars, for example, the 10-μm silicate feature has a shape very similar to that of the small silicates in the ISM; some disks have a rather steep dependence of the millimeter flux on wavelength, again typical of the small ISM grains. Some objects seem to have small silicates on the disk surface, while very large grains are implied by the millimeter spectral shape. An impressive case is that of UX Ori, which has a very peaked and strong 10-μm emission feature, typical of the small ISM amorphous silicates (Fig. 2), and an extremely flat millimeter spectrum, which may indicate the presence of very large grains in the midplane.

One should also remember that the very nature of protoplanetary disks (i.e., high optical depth, strong temperature radial gradient, etc.) prevents a complete census of the dust population, so that deriving from the observations the global properties of the solids in any given disk (such as the density of grains of different size and composition as function of radius and altitude) remains impossible for the moment, and we have to do with a piecemeal picture.

8.2. Dependence on Stellar Properties

One important step forward since *Protostars and Planets IV* has been the capability to study disks around stars of very different properties. The advent of 10-m-class telescopes on the ground, the success of Spitzer, and the improvement of the millimeter interferometers, including the VLA, have given us access to objects of increasingly lower mass. We have now millimeter spatially resolved data for TTS, and mid-IR spectra for very low mass stars and brown dwarfs, which allow us to investigate if there is a dependence of grain evolution on stellar and disk parameters. It may be worth noting that, within the millimeter-observed sample, which includes TTS and HAe stars, the stellar mass varies by a factor of 5 and the luminosity by a factor of 250; assuming typical scaling laws (*Muzerolle et al.,* 2003; *Natta et al.,* 2004b, 2006), the accretion rate in the disk is likely to vary by at least a factor of 25. The range of stellar properties is even larger for the mid-IR sample, which includes now several brown dwarfs and covers the interval between ~0.04 and 2–3 $M_\odot$ in mass, ~0.01 and 50 $L_\odot$ in luminosity, and ~10^{-10} and 10^{-6} $M_\odot$ yr in accretion rate. Over this large range of physical conditions, we do not detect *systematic* differences, i.e., grain properties do not seem to correlate with any star or disk parameter. At any given mass, there are large variations of grain properties, although objects with unprocessed grains seem to be rare.

It seems that disks around all kind of stars have the potential of processing grains, to a degree that varies for reasons not understood so far.

8.3. Time Dependence

The time dependence of grain growth is crucial information for models, and one that we would like to derive from the observations with as much detail as possible. We should stress, first of all, that there is not at present anything close to an *unbiased* sample that can be used to study grain evolution. All the observing techniques discussed in this review have been applied to selected objects, known to be suitable for detection and analysis. In addition, ages of individual pre-main-sequence stars (our best clock so far) are measured from the location on the HR diagram and have large uncertainties, especially for HAe stars and brown dwarfs. Even more importantly, the objects for which we have observations vary in age by only about a factor of 10 (from ~1 to ~10 m.y.), and individual scatter may dominate over an underlying time dependence.

The data available so far show no evidence of a correlation of the grain properties (at any wavelength) with time: We find very processed grains in the disks of the youngest as well as the oldest pre-main-sequence stars. One possible explanation is that grains are processed efficiently in the very early stages of disk evolution, when the system star + disk is still embedded and accreting actively from the natal core [see, e.g., the theoretical models of dust dynamics and evolution during the formation of a protostellar disk by *Suttner and Yorke* (2001)]. Then, the large star-to-star variation seen in, e.g., the HAe stars would be due to differences in processing during this initial, very active phase. However, we cannot exclude that further modifications also take place in the ~10 m.y. in which the disk continues to exist.

Some information can be obtained by studying grain properties in disks in Class I sources, which are in an earlier evolutionary stage than the disks around optically visible objects discussed in this review. In Class I objects, the silicate features are seen in general in absorption, and show profiles typical of small, unprocessed amorphous silicates. It is likely, however, that the absorption is dominated by grains in the surrounding envelope, for which we expect very little growth. Only if the balance between the disk emission and the intervening absorption in the core is favorable can we have a glimpse at the properties of the disk silicates, and in a few cases there is evidence that the disk silicates are much larger than those in the core (e.g., *Kessler-Silacci et al.,* 2005). Also, the young protostellar binary SVS20 in Serpens shows evidence of the 11.3-μm forsterite feature in its spectrum (*Ciardi et al.,* 2005). For the moment, there are only a few good-quality spectra, but we can expect major progress soon, as Spitzer data will become available. One would also like to know if Class I disks have millimeter spectral energy distributions as flat as those of

Class II objects. Unfortunately, using millimeter interferometry to measure the spectral index of the emission of disks embedded in Class I cores has so far proven very difficult, as the core emission is substantial even at the smallest physical scales one can probe. The extremely flat spectra of the few objects studied so far come from unresolved central condensations, and cannot be interpreted as evidence of very large grains in disks until the emission can be spatially resolved (*Hogerheijde et al.,* 1998, 1999).

8.4. Comparison with Grain Evolution Models

Models of grain growth by collisional coagulation and sedimentation (e.g., *Dullemond and Dominik,* 2005; *Weidenschilling and Cuzzi,* 1993, and references therein) predict that grain growth will occur on very short timescales. This, at first glance, is in agreement with the idea that grain properties are already changing even in the early evolutionary phases, when disks are actively accreting matter from the parental core.

However, models also predict that the growth will not stop at micrometer or even at centimeter sizes, but will proceed very quickly (compared to the pre-main-sequence stellar life times) to form planetesimals. This is not consistent with the observations, which show us disks around stars as old as 10^7 yr with grains that, albeit very large, are far from being planetesimals. When fragmentation of the conglomerates is included, in many cases the outcome is a bimodal distribution for the solids, with most of the mass in planetesimals and a tail of smaller fragments, which can be as large as centimeters and meters, but contains only a tiny fraction of the mass in planetesimals. If these smaller bodies provide sufficient optical depth, the disk properties may look similar to what is observed. However, we think this is unlikely to be the case. The millimeter observations described in section 6 tell us not only that grains need to have very big sizes but also the mass of these grains, which turns out to be very large. Using, e.g., the same grain models as in Fig. 5, we derive dust masses, for the disks with evidence of very large grains, between 10^{-3} and 10^{-2} $M_\odot$; assuming the standard gas-to-dust ratio of 100 (which is probably close to true when disks formed), this implies disk masses between ~0.1 and 1 $M_\odot$, i.e., ratios of the disk to star masses approaching unity. If a large fraction of the original dust is not in the observed population of millimeter and centimeter grains, but in planetesimals, the disk mass should be even higher, well above the gravitational instability limit. Although we cannot exclude that a *small* fraction of the original solid mass is in planetesimals, we think it is unlikely that they have collected most of it.

The survival of a large mass of millimeter- and centimeter-sized grains over a timescale of several million years, as observed in many disks, is challenging the models on several grounds. It suggests that in many cases the process of planetesimal formation is much less efficient than predicted by theoretical models. If disks are forming planetesimals as fast as predicted, then this can only happen at the end of a long quiescent phase, where growth is limited to sizes of a few centimeters at most; otherwise, the process has to be very slow, involving a modest fraction of the dust mass for most of the pre-main-sequence life of the star. The "inefficiency" may result from fragmentation of the larger bodies. This *in situ* production of the grains we observe may take care of the other severe difficulty one has, namely that millimeter and centimeter solid bodies (in a gas-rich disk) migrate toward the star on very short timescales. This is a very open field, where progress can be made only by combining together theoretical studies, laboratory experiments, and observations.

It is possible that the disks we can study with current techniques are those that will never form planets. Disks where planets form may evolve indeed very quickly, and could be below present-day detection limits. This, however, seems unlikely, as we have objects like TW Hya and HD 100546, which have evidence of very large grains in their outer disk, and an inner gap possibly due to the action of a large planet. Similar "transitional" objects are found by Spitzer in increasing number, and a detailed characterization of their millimeter properties will be important. In any case, the properties and evolution of disks that we have studied so far and their dust content provide the only observational constraints to theoretical models of grain evolution and planet formation.

8.5. Crystalline Silicates and Mineralogy

The ISO discovery of large fractional amounts of crystalline silicates in disks around stars of all masses has been a surprise. They are enhanced in the innermost regions of disks, as shown by interferometric observations of HAe stars and by the spectra of transitional disks, but they are also present, in variable degree, further out. Fractional masses of crystalline silicates, integrated over the whole disk-emitting region, have been derived for many objects, HAe, TTS, and BDs, with values ranging from zero to about 60%. These estimates refer to grains on the disk surface, typically within 10–20 AU from the star for the HAe stars, and 0.1–0.2 AU for BDs. One should note that these values are extremely model dependent, and refer to a limited range of grain sizes only; they should be taken with the greatest care. We can expect great progress in the immediate future, as spectra in the 15–45-μm spectral region, which can detect colder (and larger) crystals, are becoming available. Further insight can also come from improved characterization of the mineralogy in disks, e.g., measuring the ratio of species such as crystalline pyroxene, forsterite, silica, etc. Self-consistent radiation transfer models in disks that can include a large number of dust species exist, and can be used to provide more reliable values for the relative abundances of the various species observed on disk surfaces.

The formation of crystalline silicates requires energetic processes, which have to be efficient not only in HAe stars, where crystalline silicates were first discovered, but also in the much less luminous TTS and brown dwarfs. If crystal-

lization is restricted to the very inner disks, as in the *Gail* (2004) models, then strong radial mixing must occur, transporting material outwardly. Radial and meridian drifts can have an important role in the growth of grains, which needs to be addressed in the future.

8.6. Final Remarks

The observations we have discussed in this chapter show clearly that very few disks (if any) contain unprocessed grains, i.e., with properties similar to those of grains in the ISM. In general, dust has been largely processed in all objects.

However, the degree and the result of these changes vary a great deal from object to object, as we find large differences in the grain size, composition, and allotropic properties. At present, we have not been able to identify any correlation between the grains and other properties of the central star (such as its mass and luminosity) and of the disk (for example, mass, accretion rate, etc.), nor with the age of the system. This last point is particularly distressing, since planet formation theories require understanding if, when, and how grains change with time, or, in other words, how they "evolve."

The study of pre-main-sequence stars has shown us that, no matter which aspect of their rich phenomenology we are interested in, there is a large scatter between individuals, which can hide underlying trends. In discussing grain properties, it is possible that the objects observed so far do not sample the right range of parameters, age in particular, or that the available samples are still too small, or restricted to a too narrow range in the parameter space. We see the noise, and cannot identify trends that remain, if present, hidden. If this is really the case, we can expect major advances in the near future, as new space- and groundbased facilities will make it possible to study much larger samples of disks, in different star-forming regions, surrounding objects distributed over a broader range of mass, age, and multiplicity.

Acknowledgments. We are indebted to a number of colleagues who have provided us with unpublished material and helped in preparing some of the figures: J. Bouwman, R. van Boekel, I. Pascucci, D. Apai, J. Kessler-Silacci, J. Rodmann, M. Min, and the IRS Spitzer team. During a visit to the MPA in Heidelberg, A.N. enjoyed discussions with K. Dullemond, C. Leinert, J. Bouwman, R. van Boekel, and J. Rodmann, among others. This work was partially supported by MIUR grant 2004025227/2004 to the Arcetri Observatory.

REFERENCES

Acke B. and van den Ancker M. E. (2004) *Astron. Astrophys., 426,* 151–170.

Apai D., Pascucci I., Bouwman J., Natta A., Henning Th., and Dullemond C. P. (2005) *Science, 310,* 834–836.

Beckwith S. V. W. and Sargent A. I. (1991) *Astrophys. J., 381,* 250–258.

Beckwith S. V. W., Henning Th., and Nakagawa Y. (2000) In *Protostars and Planets IV* (V. Mannings et al., eds.), pp. 533–558. Univ. of Arizona, Tucson.

Bergin E., Calvet N., Sitko M. L., Abgrall H., D'Alessio P., et al. (2004) *Astrophys. J., 614,* L133–L136.

Bianchi S., Gonçalves J., Albrecht M., Caselli P., Chini R., Galli D., and Walmsley M. (2003) *Astron. Astrophys., 399,* L43–L46.

Blum J. (2004) In *Astrophysics of Dust* (A. N. Witt et al., eds.), pp. 369–391. ASP, San Francisco.

Calvet N., Patino A., Magris G. C., and D'Alessio P. (1991) *Astrophys. J., 380,* 617–630.

Calvet N., D'Alessio P., Hartmann L., Wilner D., Walsh A., and Sitko M. (2002) *Astrophys. J., 568,* 1008–1016.

Calvet N., D'Alessio P., Watson D. M., Franco-Hernández R., Furlan E., et al. (2005) *Astrophys. J., 630,* L185–188.

Chiang E. I. and Goldreich P. (1997) *Astrophys. J., 490,* 368–376.

Chiang E. I. and Goldreich P. (1999) *Astrophys. J., 519,* 279–284.

Ciardi D. R., Telesco C. M., Packham C., Gómez Martin C., Radomski J. T., De Buizer J. M., Phillips Ch. J., and Harker D. E. (2005) *Astrophys. J., 629,* 897–902.

Clarke C. J., Gendrin A., and Sotomayor M. (2001) *Mon. Not. R. Astron. Soc., 328,* 485–491.

D'Alessio P., Calvet N., Hartmann L., Lizano S., and Cantó J. (1999) *Astrophys. J., 527,* 893–909.

D'Alessio P., Calvet N., and Hartmann L. (2001) *Astrophys. J., 553,* 321–334.

Draine B. T. (2003) *Ann. Rev. Astron. Astrophys., 41,* 241–289.

Draine B. T. (2006) *Astrophys. J., 636,* 1114–1120.

Duchêne G., McCabe C., Ghez A. M., and Macintosh B. A. (2004) *Astrophys. J., 606,* 969–982.

Dullemond C. P. and Dominik C. (2005) *Astron. Astrophys., 434,* 971–986.

Forrest W. J., Sargent B., Furlan E., D'Alessio P., Calvet N., et al. (2004) *Astrophys. J. Suppl., 154,* 443–447.

Gail H.-P. (2004) *Astron. Astrophys., 413,* 571–591.

Guillois O., Ledoux G., and Reynaud C. (1999) *Astrophys. J., 521,* L133–L136.

Habart E., Natta A., and Krügel E. (2004a) *Astron. Astrophys., 427,* 179–192.

Habart E., Testi L., Natta A., and Carbillet M. (2004b) *Astrophys. J., 214,* L129–L132.

Habart E., Natta A., Testi L., and Carbillet M. (2006) *Astron. Astrophys., 449,* 1067–1075.

Henning Th., Michel B., and Stognienko R. (1995) *Planet. Space Sci., 43,* 1333–1343.

Henning Th., Dullemond C. P., Wolf S., and Dominik C. (2006) In *Planet Formation: Theory, Observation and Experiments* (H. Klahr and W. Brandner, eds.), pp. 112–128. Cambridge Univ., Cambridge.

Hogerheijde M. R., van Dishoeck E. F., Blake G. A., and van Langevelde H. J. (1998) *Astrophys. J., 502,* 315–336.

Hogerheijde M. R., van Dishoeck E. F., Salverda J. M., and Blake G. A (1999) *Astrophys. J., 513,* 350–369.

Jayawardhana R., Hartmann L., Fazio G., Fisher R. S., Telesco C. M., and Piña R. K. (1999) *Astrophys. J., 521,* L129–L132.

Jensen E. L. N. and Mathieu R. D. (1997) *Astron. J., 114,* 301–316.

Keller L. P., Hony S., Bradley J. P., Molster F. J., Waters L. B. F. M., et al. (2002) *Nature, 417,* 148–150.

Kemper F., Vriend W. J., and Tielens A. G. G. M. (2004) *Astrophys. J., 609,* 826–837.

Kessler-Silacci J. E., Hillenbrand L. A., Blake Geoffrey A., and Meyer M. R. (2005) *Astrophys. J., 622,* 404–429.

Kessler-Silacci J. E., Augereau J.-C., Dullemond C. P., Geers V., Lahuis F., et al. (2006) *Astrophys. J., 639,* 275–291.

Krügel E. and Siebenmorgen R. (1994) *Astron. Astrophys., 288,* 929–941.

Lucas P. W., Fukagawa M., Tamura M., Beckford A. F., Itoh Y., et al. (2004) *Mon. Not. R. Astron. Soc., 352,* 1347–1364.

Marsh K. A. and Mahoney M. J. (1992) *Astrophys. J., 395,* L115–L118.

McCabe C., Duchêne G., and Ghez A. M. (2003) *Astrophys. J., 588,* L113–L116.

McCaughrean M. J., Stapelfeldt K. R., and Close L. M. (2000) In *Protostars and Planets IV* (V. Mannings et al., eds.), pp. 485–507. Univ. of Arizona, Tucson.

Meeus G., Waters L. B. F. M., Bouwman J., van den Ancker M. E., Waelkens C., and Malfait K. (2001) *Astron. Astrophys., 365,* 476–490.
Meeus G., Sterzik M., Bouwman J., and Natta A. (2003) *Astron. Astrophys., 409,* L25–L29.
Menshchikov A. B. and Henning Th. (1997) *Astron. Astrophys., 318,* 879–907.
Min M., Hovenier J. W., de Koter A., Waters L. B. F. M., and Dominik C. (2005) *Icarus, 179,* 158–173.
Min M., Dominik C., Hovenier J. W., de Koter A., and Waters L. B. F. M. (2006) *Astron. Astrophys., 445,* 1005–1014.
Miyake K. and Nakagawa Y. (1993) *Icarus, 106,* 20–41.
Miyake K. and Nakagawa Y. (1995) *Astrophys. J., 441,* 361–384.
Muzerolle J., Calvet N., Briceño C., Hartmann L., and Hillenbrand L. (2000) *Astrophys. J., 535,* L47–L50.
Muzerolle J., Hillenbrand L., Calvet N., Briceño C., and Hartmann L. (2003) *Astrophys. J., 592,* 266–281.
Muzerolle J., Megeath S. T., Gutermuth R. A., Allen L. E., Pipher J. L., et al. (2004) *Astrophys. J. Suppl., 154,* 379–384.
Muzerolle J., Adame L., D'Alessio P., Calvet N., Luhman K. L., et al. (2006) *Astrophys. J., 643,* 1003–1010.
Natta A. and Testi L. (2004) In *Star Formation in the Interstellar Medium: In Honor of David Hollenbach, Chris McKee and Frank Shu* (D. Johnstone et al., eds.), pp. 279–285. ASP, San Francisco.
Natta A., Testi L., Neri R., Shepherd D. S., and Wilner D. J. (2004a) *Astron. Astrophys., 416,* 179–186.
Natta A., Testi L., Muzerolle J., Randich S., Comerón F., and Persi P. (2004b) *Astron. Astrophys., 424,* 603–612.
Natta A., Testi L., and Randich S. (2006) *Astron. Astrophys.,* in press (astro-ph/0602618).
Ossenkopf V. and Henning Th. (1994) *Astron. Astrophys., 291,* 943–959.
Peeters E., Hony S., Van Kerckhoven C., Tielens A. G. G. M., Allamandola L. J., Hudgins D. M., and Bauschlicher C. W. (2002) *Astron. Astrophys., 390,* 1089–1113.
Pollack J. B., Hollenbach D., Beckwith S., Simonelli D. P., Roush T., and Fong W. (1994) *Astrophys. J., 421,* 615–639.
Przygodda F., van Boekel R., Ábrahám P., Melnikov S. Y., Waters L. B. F. M., and Leinert Ch. (2003) *Astron. Astrophys., 412,* L43–L46.
Qi C., Ho P. T. P., Wilner D. J., Takakuwa S., Hirano N., et al. (2004) *Astrophys. J., 616,* L11–L14.
Quillen A. C., Blackman E. G., Frank A., and Varnière P. (2004) *Astrophys. J., 612,* L137–L140.
Ressler M. E. and Barsony M. (2003) *Astrophys. J., 584,* 832–842.
Rice W. K. M., Wood K., Armitage P. J., Whitney B. A., and Bjorkman J. E. (2003) *Mon. Not. R. Astron. Soc., 342,* 79–85.
Rodmann J., Henning Th., Chandler C. J., Mundy L. G., and Wilner D. J. (2006) *Astron. Astrophys., 446,* 211–223.
Sargent B., Forrest W. J., D'Alessio P., Najita J., Li A., et al. (2005) Poster presented at IAU Symp. 231 on "Astrochemistry Throughout the Universe: Recent Successes and Current Challenges," Asilomar, California.
Sargent B., Forrest W. J., D'Alessio P., Li A., Najita J., et al. (2006) *Astrophys. J.,* in press (astro-ph/0605415).
Schräpler R. and Henning Th. (2004) *Astrophys. J., 614,* 960–978.
Shuping R. Y., Bally J., Morris M., and Throop H. (2003) *Astrophys. J., 587,* L109–L112.
Sicilia-Aguilar A., Hartmann L., Calvet N., Megeath S. T., Muzerolle J., et al. (2006) *Astrophys. J., 638,* 897–919.
Sloan G. C., Keller L. D., Forrest W. J., Leibensperger E., Sargent B., et al. (2005) *Astrophys. J., 632,* 956–963.
Suttner G. and Yorke H. W. (2001) *Astrophys. J., 551,* 461–447.
Testi L., Natta A., Shepherd D. S., and Wilner D. J. (2001) *Astrophys. J., 554,* 1087–1094.
Testi L., Natta A., Shepherd D. S., and Wilner D. J. (2003) *Astron. Astrophys., 403,* 323–328.
Throop H. B., Bally J., Esposito L. W., and McCaughrean M. J. (2001) *Science, 292,* 1686–1689.
Uchida K. I., Calvet N., Hartmann L., Kemper F., Forrest W. J., et al. (2004) *Astrophys. J. Suppl., 154,* 439–442.
van Boekel R., Min M., Leinert Ch., Waters L. B. F. M., Richichi A., et al. (2004a) *Nature, 432,* 479–482.
van Boekel R., Waters L. B. F. M., Dominik C., Dullemond C. P., Tielens A. G. G. M., and de Koter A. (2004b) *Astron. Astrophys., 418,* 177–184.
van Boekel R., Min M., Waters L. B. F. M., de Koter A., Dominik C., van den Ancker M. E., and Bouwman J. (2005) *Astron. Astrophys., 437,* 189–208.
van Diedenhoven B., Peeters E., Van Kerckhoven C., Hony S., Hudgins D. M., Allamandola L. J., and Tielens A. G. G. M. (2004) *Astrophys. J., 611,* 928–939.
Van Kerckhoven C., Tielens A. G. G. M., and Waelkens C. (2002) *Astron. Astrophys., 384,* 568–584.
Voshchinnikov N. V. and Krügel E. (1999) *Astron. Astrophys., 352,* 508–516.
Voshchinnikov N. V., Ilin V. B., Henning Th., and Dubkova D. N. (2006) *Astron. Astrophys., 445,* 167–177.
Weidenschilling S. J. and Cuzzi J. N. (1993) In *Protostars and Planets III* (E. H. Levy and J. N. Lunine, eds.), pp. 1031–1060. Univ. of Arizona, Tucson.
Weingartner J. C. and Draine B. T. (2001) *Astrophys. J., 548,* 296–309.
Wilner D. J., Ho P. T. P., Kastner J. H., and Rodríguez L. F. (2000) *Astrophys. J., 534,* L101–104.
Wilner D. J., D'Alessio P., Calvet N., Claussen M. J., and Hartmann L. (2005) *Astrophys. J., 626,* L109–L112.
Wurm G., Paraskov G., and Krauss O. (2005) *Icarus, 178,* 253–263.